Bewertung von aktiven und passiven Schaltentlastungstechniken für Anwendungen in Hochsetzstellern zur Leistungsfaktorkorrektur
Evaluation of Active and Passive Snubber Techniques for Applications in Power-Factor-Correction Boost Converters

Milan M. Jovanovic, Chen Zhou und Peter Liao, Delta Power Electronics Lab., Blacksburg, VA/USA

Zusammenfassung – Die Vorzüge und Grenzen von einer nullspannungsschaltenden (ZVS), aktiven Schaltentlastungstechnik und verlustlosen, passiven Shaltentlasungstechnik werden für Anwendungen in Hochsetzstellern (boost-Topologien) zur Leistungsfaktorkorrektur im nichtlückenden Betrieb untersucht. Die Techniken werden hinsichtlich ihrer Komplexität, ihres Wirkungsgrades and Storm- und Spannungsbelastungen der Halbleiterelemente bewertet. Die Versuchsergebnisse des bewertenden Vergleichs werden ebenfalls gezeigt.

Abstract – Merits and limitations of a zero-voltage-switching (ZVS) based active-snubber technique and a lossless passive-snubber technique are evaluated for applications in continuous-conduction-mode, power-factor-correction boost converters. The techniques are evaluated based on their complexity, efficiency, and voltage and current stresses on the semiconductor components. The experimental results of the evaluations are also presented.

1 Introduction

With ever-increasing demand for power from the ac line and more stringent requirements for power quality, power-factor correction (PFC) is becoming an integral part of power supplies. A variety of topologies are available for PFC [1, 2, 3]. While dicontinuous-mode converters are well suited for low-power applications, peak-and average-mode controlled boost converters operating in continuous-conduction mode (CCM) are still the primary choice for many medium and high-power applications [1, 4].

Generally, the efficiency and the maximum switching frequency of the conventional PWM CCM boost converter are limited by the reverse-recovery loss of the output rectifier. To reduce or even eliminate this loss, the rate of change of the rectifier current during turnoff must be slowed down. The required rectifier-current wave shaping can be achieved by either active or passive snubbers [5, 6, 7, 8]. Generally, active snubbers consist of an auxiliary switch with a few passive components that are used to control di/dt rate of the rectifier current and to create conditions for zero-voltage switching (ZVS) of the main switch and the rectifier [5, 6]. A potential drawback of the active-snubber approaches is a need for an additional switch with current and voltage ratings comparable to

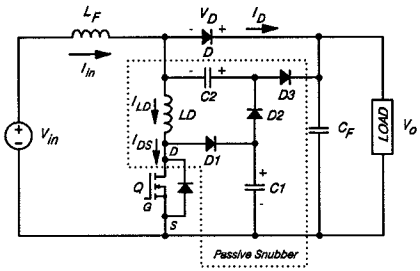

Fig. 1: Circuit diagram of boost converter with passive snubber.

those of the main switch and its associated gate drive. Therefore, lossless snubber techniques that use only passive components are attractive from the cost point of view.

In this paper, a thorough evaluation of a simple passive lossless snubber technique and the ZVS active-snubber technique introduced in [6] is presented. The evaluation focuses on relative comparisons of these two approaches with respect to their efficiency (performance), current and voltage stresses on their semiconductor components (reliability), and complexity (cost). The comparisons are performed on an experimental 600-W boost converter.

2 Passive Snubber

The circuit diagram of the boost converter with the passive, lossless snubber evaluated in this work is shown in Fig 1. The snubber consists of inductor L_D, capacitors C_1 and C_2, and diodes D_1, D_2, and D_3. Since inductor L_D is connected in series with transistor Q and rectifier D, its value can be used to control the reverse-recovery characteristic of the rectifier by controlling the rectifier di/dt rate [9].

To facilitate the explanation of the operation of the circuit, Fig. 2 show the key waveforms. The waveforms in Fig. 2 are obtained by a Spice simulation assuming that $C_1 = C_2$. The basic principle of operation does not change if the capacitor values are different.

To simplify the analysis of operation, it is assumed that all the components in the circuit are ideal, and that inductance L_F is large enough to be modeled as a constant-current source (I_{in}).

Before transistor Q is turned on at $t = T_0$, only diode D is conducting. At the same time, capacitor C_2 is fully discharged, i.e., $V_{C2} = 0$, while capacitor C_1 is charged up to $V_{C1} = V_0$. When the transistor is turned on at $t = T_0$, inductor current i_L starts increasing. Since during this time rectifier D is still conducting the current difference $I_{in} - i_L$, the voltage across the inductor is clamped to V_0, as can be seen from the equivalent circuit shown in Fig. 3(a). As a result, during this topological stage, diodes D_1, D_2, and D_3 are off.

The rate of change of the rectifier current is determined by V_0/L_D. By controlling this rate through a proper selection of the L_D value, the recovered charge of the rectifier can be controlled, too. Generally, a slower rate of current change results in a smaller recovered charge [9].

Rectifier D ceases to conduct at $t = T_1$ when current i_L becomes equal to input current I_{in}. At the same time, diode D_2 starts conducting, and C_1, C_2, and L_D form a series-resonant circuit, as shown in Fig. 3(b). Due to the presence of diode D_2, this circuit can conduct current only in one direction. As a result, during the $T_1 - T_2$ interval, the charge from C_1 is transferred to C_2 in a resonant manner. The voltage across C_2 at the end of the resonant interval is equal to the voltage of C_1 at the beginning of the resonant interval. Therefore, at $t = T_2$, $V_{C1} = 0$ and $V_{C2} = V_0$. The peak of the resonant current, which determines the current stress of the transistor is equal to $I_{pk} = V_0/Z_n$, where $Z_n = \sqrt{L_D(C_1 + C_2)/C_1C_2}$ is the characteristic impedance of the resonant tank.

During the $T_2 - T_3$ interval, all the diodes are off, and constant input current I_{in} is flowing through the switch, as shown in Fig. 3(c). When, at $t = T_3$, the transistor is turned off, the transistor current is diverted

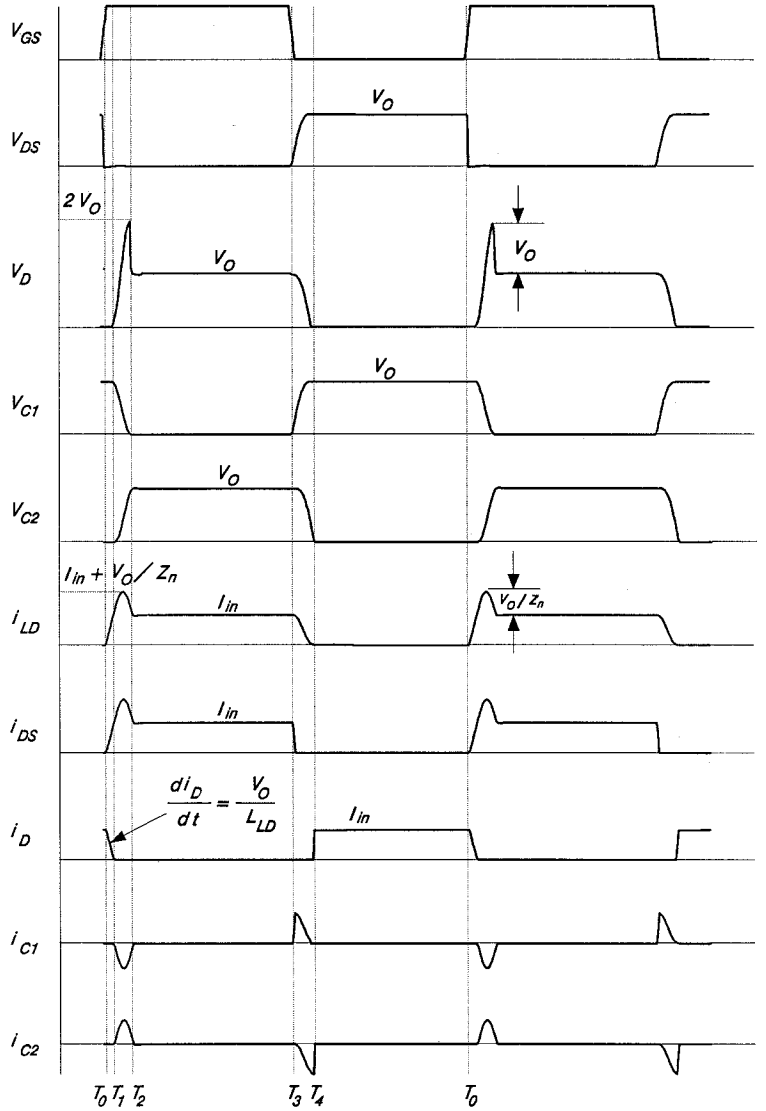

Fig. 2: Key waveforms of ideal boost converter with passive snubber for $C_1 = C_2$.

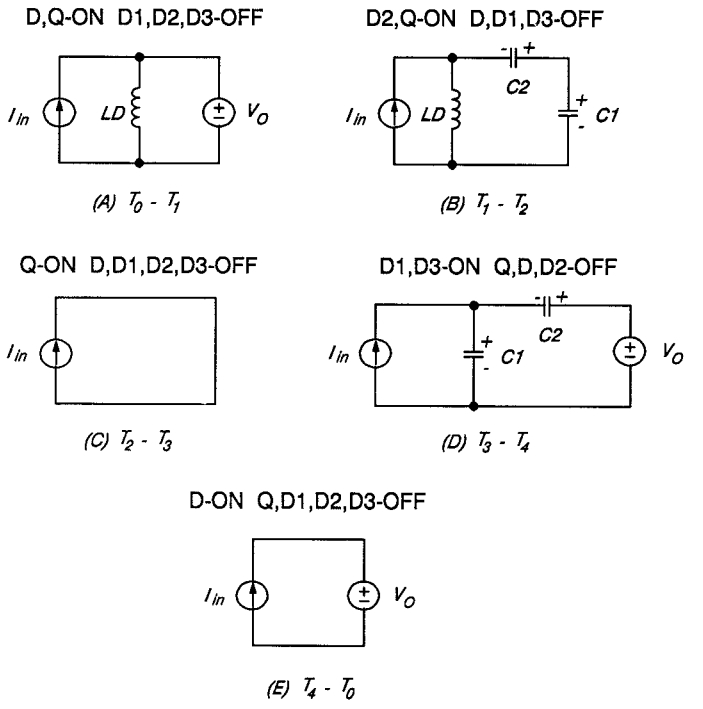

Fig. 3: Equivalent circuits of passive-snubber topological stages.

into C_1 and C_2, as shown in Fig. 3(d). Capacitor C_1 starts charging toward V_0, while capacitor C_2 starts discharging toward zero through conducting diode D_3. At $t = T_4$, $V_{C2} = 0$ and rectifier D starts conducting as shown in Fig. 3(e). At $t = T_0$, the transistor is turned on again, and the circuit enters the next switching cycle.

When the circuit parasitics, primarily diode junction capacitance, are taken into consideration, the basic circuit operation remains unchanged. The most noticeable effect of the parasitics is observed on the rectifier voltage V_D, which shows low-energy, high-frequency ringings. These ringings can be easily suppressed by a low-power RC snubber placed across the rectifier.

As can be seen from Fig. 2, the addition of the snubber does not change the voltage stress of the transistor, which is $V_{DS(max)} = V_0$. However, the voltage stress on the diode is $V_{D(max)} = 2V_0$, and it is twice the stress when the circuit is operating without the snubber. On the other hand, the snubber does not change the diode current stress ($I_{D(max)} = I_0$), but increases the transistor current stress from $I_{DS(max)} = I_0$ without the snubber to $I_{DS(max)} = I_0 + V_0/Z_n$ with the snubber.

Since the voltage stress on the diode is independent of the values of the snubber's reactive components C_1, C_2, and L_D, it cannot be reduced by a snubber design op-

timization. The only way to reduce this stress is to place snubber inductor L_D directly in series with rectifier D rather than with transistor Q. However, this change would double the voltage stress on the transistor.

The current stress of the transistor can be minimized by maximizing characteristic impedance Z_n. Since the value of L_D is determined from the desired rate of change of the rectifier current, the characteristic impedance can be maximized by minimizing the equivalent series capacitance of C_1 and C_2. However, the lower limit on the value of the snubber capacitances is determined by their energy-storage capacity. Namely, capacitor C_1, at V_0, ought to be able to store the energy at least equal to the energy in the snubber inductor at the moment of turn-off, i.e., $1/2C_1V_0^2 > 1/2L_DI_{in}^2$. Otherwise, the excessive inductor energy would flow through D_1, D_2, and D_3 directly to the load. This is not desirable, since diodes $D_1 - D_3$ may introduce severe reverse-recovery problems.

3 ZVS Active Snubber

Recently, a new class of zero-voltage-transition (ZVT) PWM converters, which overcome some deficiencies of the existing soft-switched converters, has been introduced [6]. By using a resonant network with an auxiliary switch, the converters of this family achieve ZVS for both the main switch and the rectifier without increasing their voltage and current stresses. Due to the soft switching of the rectifier that virtually eliminates the problems related to the reverse recovery, this technique seems suitable for applications in high-power, PFC boost converters. Figure 4 shows the circuit diagram of the ZVT-PWM boost power stage, while Fig. 5 shows its key waveforms [6].

In the ZVT-PWM boost power stage in Fig. 4, an additional resonant network consisting of resonant inductor L_R, auxiliary switch S_1, and diode D_1 is added. Due to applying the capacitor-shift rule, rectifier

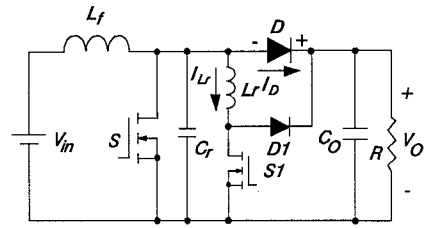

Fig. 4: Circuit diagram of ZVT-PWM boost power stage.

capacitance C_D can be placed across C_R so that it becomes part of C_R. To simplify the analysis, the input filter inductance is assumed large enough to be considered as a constant current source.

As shown in Fig. 6, the converter goes through seven topological stages during a conversion cycle. Prior to $t = T_0$, main switch S and auxiliary switch S_1 are off, while rectifier D is conducting. At $t = T_0$, S_1 is turned on and current i_L starts flowing through L_R. The equivalent circuit during this topological stage is shown in Fig. 6(a). Due to the constant voltage across the inductor, i_L increases linearly until, at $t = T_1$, it reaches I_{in}, when rectifier D is turned off with soft switching.

During the $T_1 - T_2$ interval, all semiconductor switches except auxiliary switch S_1 are off so that L_R and C_R form a resonant circuit. I_L continues to increase in a resonant manner, while C_R starts discharging. When, at $t = T_2$, the voltage across C_R becomes zero, the anti-parallel diode of main switch S starts conducting, as shown in Fig. 6(c). To obtain ZVS, the turn-on signal should be applied to switch S while its body diode is conducting. During the $T_2 - T_3$ interval, i_L stays constant because the inductor is shorted.

At $t = T_4$, switch S_1 is turned off and i_L is diverted from S_1 to D_1 as shown in Fig. 6(d). Due to the conduction of D_1, the voltage across switch S_1 is clamped to V_0. During this stage, the resonant-inductor cur-

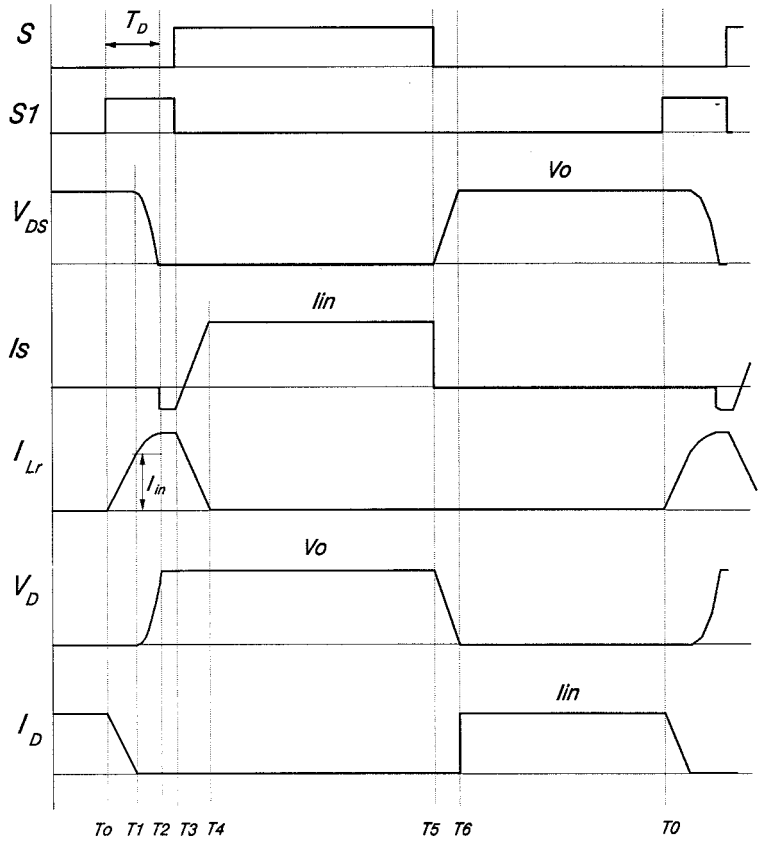

Fig. 5: Key waveforms of ZVT-PWM boost power stage.

rent decreases linearly, and the inductor energy is transferred to the output. When i_L becomes zero at $t = T_4$, diode D_1 turns off.

In the following interval, $T_4 - T_5$, main switch is on, while all the other semiconductors are off. The input current flows through switch S until the switch is turned off at $t = T_5$, when the current is diverted into resonant capacitor C_R as shown in Fig. 6(f). Because of constant input current I_{in}, the voltage across C_R increases linearly until it reaches V_0 at $t = T_6$, when rectifier D starts conducting as shown in Fig. 6(g). This stage is terminated at $t = T_0$, when switch S_1 is turned on and a new conversion cycle is initiated.

As can be seen from the above analysis, the main switch and the rectifier are "softly switched". The main switch is turned on at zero voltage, while the rectifier is turned off at zero voltage. As a result, the turn-on switching loss of the switch is eliminated. In addition, due to the controlled di/dt rate and soft switching of the rectifier, its reverse-recovery characteristic is greatly improved. Also, the current and voltage stresses on the main switch and the rectifier are the same as in the conventional,

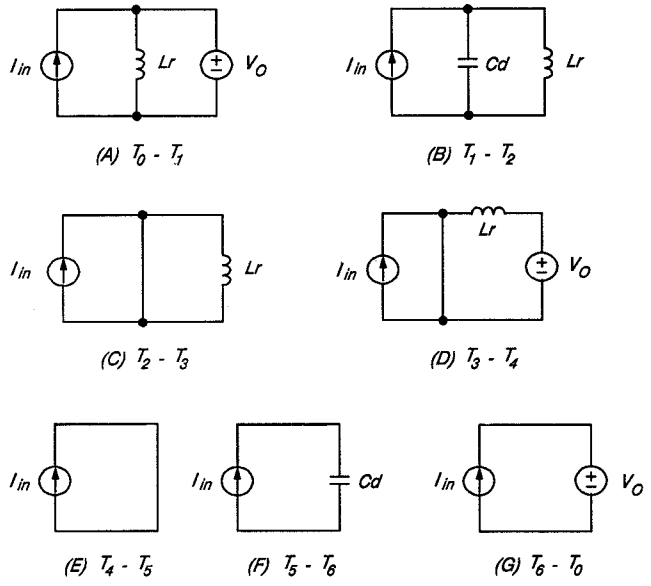

Fig. 6: Equivalent circuits of active-snubber boost converter topological stages.

single-switch circuit.

In this converter, the auxiliary switch is forced ("hard") commutated. The switch is turned on when the current, which is greater than the input current, is flowing through the switch. Consequently, this switch suffers from the turn-on switching loss and conduction loss. However, since the auxiliary switch conducts only during a brief time around the turn-on transitions of the main switch, it handles a small amount of power compared to the main switch. Therefore, the conduction loss of the switch is relatively small. In addition, if the auxiliary switch is selected with a relatively small output capacitance, its turn-on switching loss is also small. Usually, this relatively small power loss on the auxiliary switch is more than offset by the reduction of the power loss due to the improved reverse-recovery characteristic of the rectifier.

It should be noted that the boost circuit described in [5] has the same features as the above-analyzed converter. However, the implementations of the active snubber circuits slightly differ in these two circuits. The circuit described in this section requires fewer components. In addition, it is only one member of a larger converter family of ZVT-PWM converters. The approach described in [5] is only introduced to alleviate problems associated with the reverse-recovery characteristics of the rectifier in the boost converter.

4 Evaluation Results

The experimental evaluation of the described passive and active snubber was performed on a 600-W, PFC boost converter with average current-mode control. The converter was designed for the 90-260-Vac input-voltage range, and with the output voltage of 380 Vdc. Figure 7 shows the circuit diagram of the experimental converter with the active snubber.

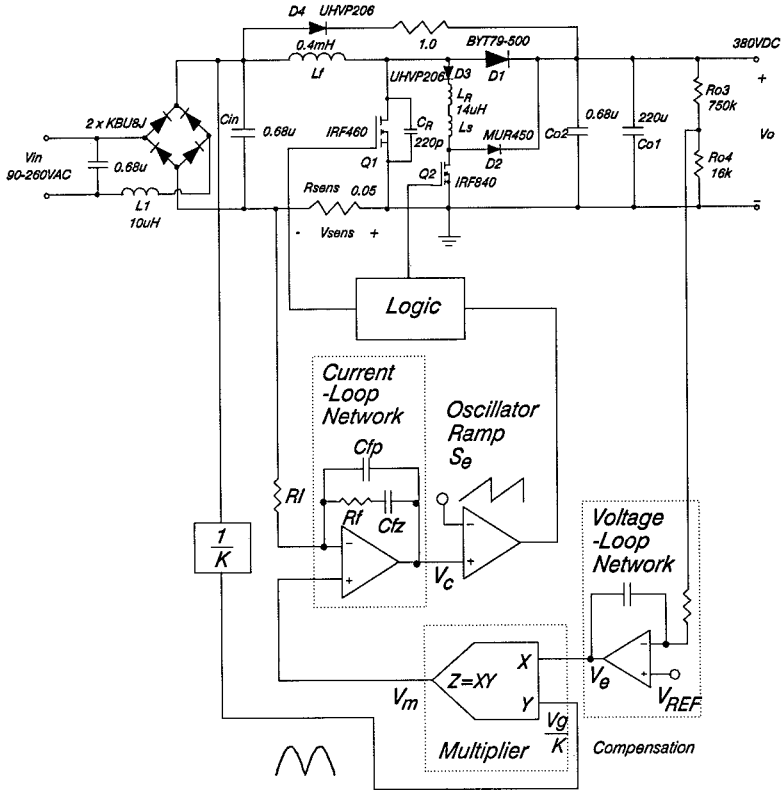

Fig. 7: Experimental, 600-W, ZVT-PWM boost converter.

The efficiency of the converter without the snubber (i.e., when S_1, L_R, C_R, L_S, and D_1 are removed from the circuit) as a function of the input voltage is shown in Fig. 8 for different rectifiers [9, 10]. Rectifiers BYT79-500 and HFA15TB60 are available on the market [9, 10], while the rectifier labeled HEXFRED10 is in the development stage at IR. As can be seen, the ultra-fast HEXFRED10 rectifier results in the best efficiency of the converter, which ranges from 91% at low line up to 98% at high line. The HFA15TB60 rectifier achieves the same efficiency at low line, but slightly lower (97.5%) at high line. The measured efficiency for the BYT79-500, which among the tested diodes has the longest recovery time, was in the 89% - 97.5% range. The measured efficiency of the converter with the active snubber is shown in Fig. 9. Due to a controlled di/dt rate and ZVS of the rectifier, the efficiency of the converter is almost insensitive to the reverse-recover speeds of the rectifiers. The maximum difference in efficiency for the three diodes, which occurs at high line, is less than 0.5%, which is within the measurement error range. It also should be noted that the minimum ef-

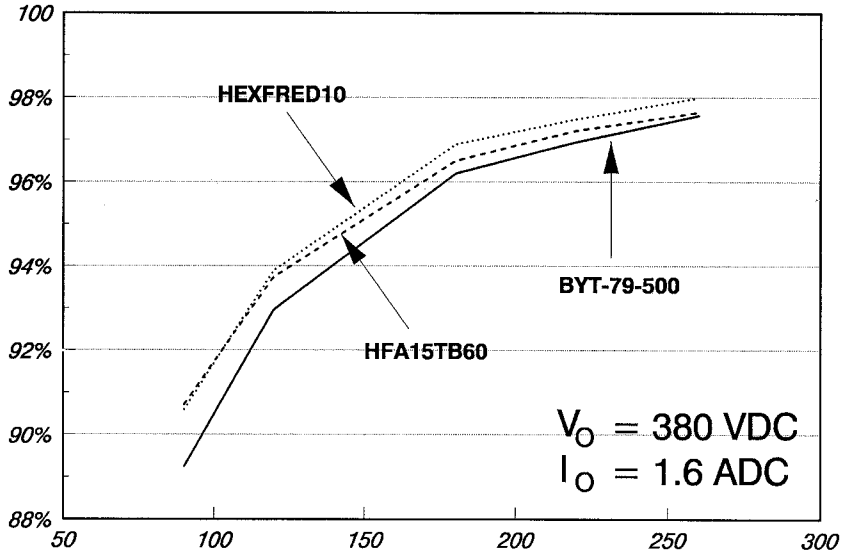

Fig. 8: Measured efficiency as a function of input voltage of converter without snubber.

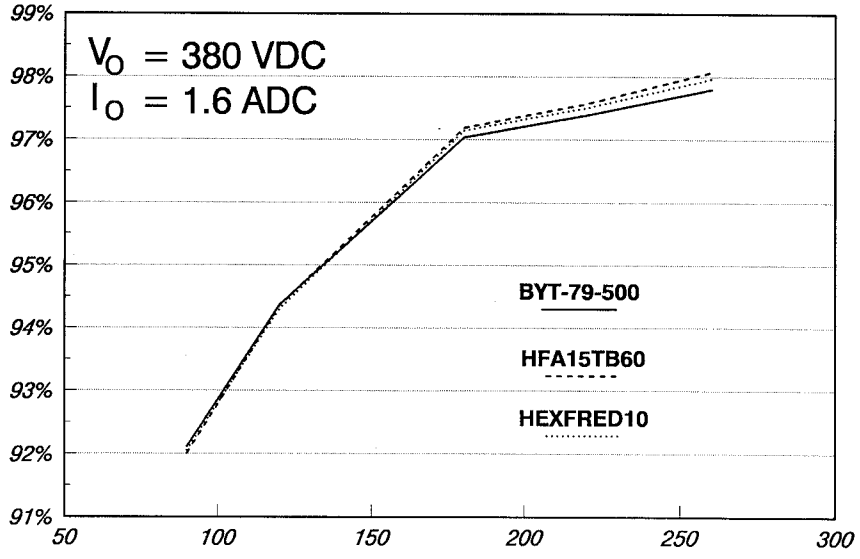

Fig. 9: Measured efficiency as a function of input voltage of converter with active snubber.

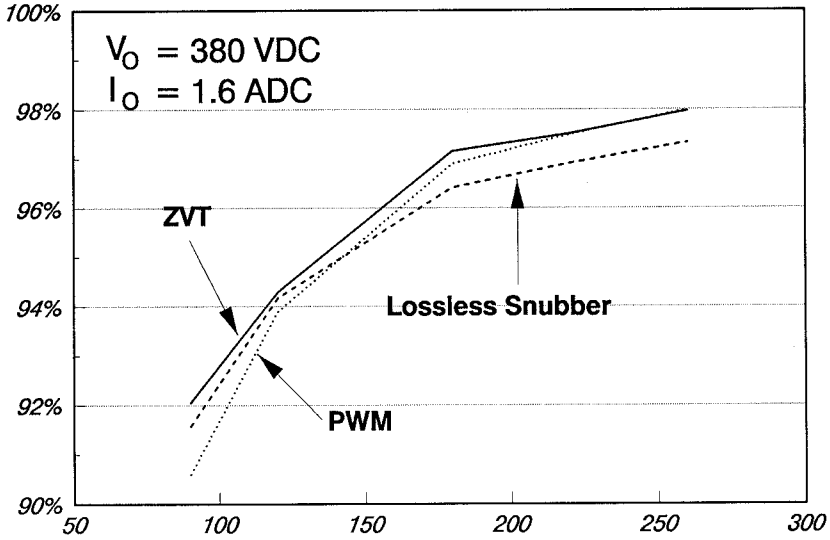

Fig. 10: Comparison of measured efficiencies as functions of input voltage of converters with passive, active, and without snubber.

ficiency that occurs at low line is increased to 92%. This represents approximately 3% increase with respect to the circuit with BYT79-500. The maximum efficiency is not affected by the active snubber. At 98%, it is the same as for the converter without the snubber.

Finally, Fig. 10 shows the measured efficiency of the converter without a snubber and with active and passive snubber. In this evaluation, the HEXFRED10 rectifier is used in all the three circuits. It should be noted that the converter with the passive snubber requires a rectifier with at least 800-V rating (twice the output voltage). Although the HEXFRED10 device is rated at 600 V, we could use this device in our evaluations because our samples exhibited the breakdown voltages in excess of 800 V.

The converter with the passive snubber is obtained from the circuit shown in Fig. 7 by removing the active-snubber components and inserting the following passive-snubber components according to Fig. 1: $C_1 = C_2$=3.3 nF, L_D= 2.5 μH, and $D_1 - D_3$ = MUR450.

As can be seen, at low line the efficiency of the converter with the passive snubber is only 0.5% lower than that of the converter with the active snubber. At high line the efficiency of the passive-snubber converter is 1% lower than the efficiency of the active-snubber converter. This is mainly due to the snubber loss. However, since the minimum efficiency dictates the thermal design, the same thermal design is required for both the active- and passive-snubber converters.

Although efficiency-wise the ZVT circuit has a slight edge over the converter with the passive snubber, its major advantages are in a much lower voltage stress on the rectifier and virtually ringing-free waveforms. These two features are usually translated into a more reliable operation and smaller-size EMI filters of the ZVT converter.

The number of power-stage components in the ZVT converter and in the converter

with passive snubber is almost the same. As a result, the sizes of the two circuits are similar.

Finally, the cost of the auxiliary switch and its associated gate drive in the ZVT circuit is more than justified by the overall performance improvements at high-power levels. This is especially true for the power levels in the kW range and beyond.

5 Summary

Comparisons between the ZVS passive-snubber technique and the active-snubber technique based on the newly introduced zero-voltage-transition (ZVT) principle were presented. The merits and limitations of these techniques were evaluated with respect to their performance, current and voltage stresses of their semiconductor components, and complexity.

It was shown that both techniques improve the conversion efficiency. The active-snubber approach results in a slightly higher efficiency. However, the main advantages of the active-snubber technique is a much smaller voltage stress on the rectifier and very smooth, ringing-free waveforms. These features make this approach very attractive at high power levels, and more than justify the cost of the auxiliary switch and its associated gate drive.

Acknowledgements

The authors wish to thank Mr. Guichao Hua of Virginia Power Electronics Center (VPEC) at Virginia Tech, Blacksburg, for providing the original Freelance files for figures included in Sec. 3, and to VPEC for providing the evaluation PCB for the ZVT-PWM, PFC boost converter.

References

[1] M.K. Nalbant, A. Koblinski, "Active power factor correction technique," *Application Note 9, Micro Linear Data Book,* 1990.

[2] L. Dixon, "High power factor preregulators for off-line supplies," *Unitrode Power Supply Design Seminar Manual,* SEM-700, 1990.

[3] C. Zhou, R.B. Ridley, F.C. Lee, "Design and analysis of a hysteretic boost power factor correction circuit," *IEEE Power Electronics Specialists' Conf. Rec.,* pp. 800-807, 1990.

[4] L. Dixon, "Average current mode control of switching power supplies," *Unitrode Power Supply Design Seminar Manual,* SEM-700, 1990.

[5] R. Streit, D. Tollik, "High efficiency telcom rectifier using a novel soft-switched boost-based input current shaper," *International Telecommunication Energy Conf. Proc.,* pp. 720 - 726, 1991.

[6] G. Hua, C.S Leu, F.C. Lee, "Novel zero-voltage-transition PWM converters," *IEEE Power Electronics Specialists' Conf. Rec.,* pp. 55-61, 1992.

[7] T. Ninomiya, N. Matsumoto, K. Hasrada, R. Hiromatsu, "Noise suppression by magnetic snubbers in switching power converters," *IEEE Power Electronics Specialists' Conf. Rec.*, pp. 1133 - 1140, 1988.

[8] C.L. Rym, P.V. Bury, "Power growth of switching power FET structure in hybrid technology: application to spaceborn converters," *IEEE Power Electronics Specialists' Conf. Rec.,* pp. 234 - 241, 1985.

[9] Y. Khersonsky, M. Robinson, D. Gutierrez, "New fast recovery diode technology cuts circuit losses, improves reliability," *Power Conversion & Intelligent Motion (PCIM) Magazine,* pp. 16 - 25, May 1992.

[10] Philips, "Rectifier Diodes and Thyristors," *Data Handbook A1,* pp. 233 - 242, 1988.